Theoretical Study of Spin Crossover in 30 Iron Complexes

Kepp, Kasper Planeta

Published in:
Inorganic Chemistry

Link to article, DOI:
10.1021/acs.inorgchem.5b02371

Publication date:
2016

Document Version
Peer reviewed version

A Theoretical Study of Spin Crossover in 30 Iron Complexes

Kasper P. Kepp*

Technical University of Denmark, DTU Chemistry, Building 206, 2800 Kgs. Lyngby, DK – Denmark.

* Corresponding Author. Phone: +045 45 25 24 09. E-mail: kpj@kemi.dtu.dk

Abstract

Iron complexes are important spin crossover (SCO) systems with vital roles in oxidative metabolism and promising technological potential. The SCO tendency depends on the free energy balance of high- and low-spin states, which again depends on physical effects such as dispersion, relativistic effects, and vibrational entropy. This work studied 30 different iron SCO systems with experimentally known thermochemical data, using 12 different density functionals. Remarkably general entropy-enthalpy compensation across SCO systems was identified (R = 0.82, p = 0.002) that should be considered in rational SCO design. Iron(II) complexes displayed higher ΔH and ΔS values than iron(III) complexes and also less steep compensation effects. First-coordination sphere ΔS values computed from numerical frequencies reproduce most of the experimental entropy and should thus be included when modeling spin-state changes in inorganic chemistry (R = 0.52, p = 3.4 x 10^{-3}; standard error in TΔS ~ 4.4 kJ/mol at 298 K vs. 16 kJ/mol of total TΔS on average). Zero-point energies favored high-spin states by 9 kJ/mol on average. Interestingly, dispersion effects are surprisingly large for the SCO process (average: 9 kJ/mol, but up to 33 kJ/mol) and favor the more compact low-spin state. Relativistic effects favor low-spin by ~9 kJ/mol on average, but up to 24 kJ/mol. B3LYP*, TPSSh, B2PLYP, and PW6B95 performed best for the typical calculation scheme that includes ZPE. However, if relativistic and dispersion effects are included, only B3LYP* remained accurate. On average, high-spin was favored by LYP by 11−15 kJ/mol relative to other correlation functionals, and by 4.2 kJ/mol per 1% HF exchange in hybrids. 13% HF exchange was optimal without dispersion and 15% was optimal with all effects included for these systems.

Keywords: spin crossover, iron complexes, DFT, entropy, relativistic effects, dispersion.

Introduction.

The interchange between spin states of iron complexes, an intrinsically quantum-mechanical phenomenon, is a vital feature ensuring biological control over the triplet dioxygen of our atmosphere[1,2] and this interchange also forms the basis of many technological applications within diverse areas of molecular electronics[3,4,5] and transition-metal-based catalysis[6,7]. The interchange is determined by the free energy difference of high-spin (HS) and low-spin (LS) states[8,9], which depends on both the metal ion and the ligands bound to it, as typified by the spectrochemical series[10,11].

Many spin-crossover (SCO) systems containing iron have been designed during the past many decades, and for a range of them, the free energy has been decomposed into entropy (ΔS) and enthalpy (ΔH) contributions[3,5]. HS states tend to have longer metal-ligand bond lengths and thus larger vibrational entropy due to the occupation of the e_g orbitals, and this entropy effect dominates the total entropy difference between the states and is largely responsible for the thermally induced transition to HS observed experimentally, as the $T\Delta S$ term begins to favor the HS state[3,8].

Yet, in computational inorganic chemistry the $T\Delta S$ contribution is often overlooked, despite being a major contribution to the reason we observe HS states in catalytic and enzymatic intermediates and ground states of coordination complexes[9]. There is thus a need to consider whether we can include this entropy accurately. The spin state balance is also very sensitive to the theoretical method used to describe it, one of the major challenges in the field of theoretical inorganic chemistry, with the standard density functionals providing highly variable results[12,13,14,15,16,17,18,19,20,21,22,23,24,25,26,27], and alternative methods such as CASPT2[22,28] and density matrix renormalization group calculations[29] can also be used to assess the electronic structures of such compounds.

Also, despite the ongoing research into new and highly promising SCO systems[4,30,31,32,33,34], we do not yet understand the physics of SCO well enough to rationally predict SCO behavior in a new

class of compounds. This is mainly because, in addition to the important effect of TΔS, which is half of the equation in terms of predicting SCO behavior accurately, there are potential contributions from zero-point energies (ZPE), relativistic effects, and dispersion whose magntitudes, directions, and system-dependencies, e.g. long-range effects in lattices, which are not systematically understood[9], although recent research effects have shown substantial advances on the environment aspect of the SCO process[26,35,36,37,38].

Three questions of scientific interest will be addressed in this paper, notably i) how well does the first coordination sphere alone describe the thermodynamics of SCO? ii) how much do relativistic effects and dispersion contribute to the process? and iii) what is the nature of the interplay between ΔS and ΔH and the molecular interpretations, and is this interplay generic? A fourth, practical question to be addressed is: Can we actually model both ΔS and ΔH accurately?

To address these questions, this paper reports a systematic study of 30 thermochemically characterized iron SCO complexes, referred to below as the 30SCOFE data set, the largest data set of SCO systems so far studied. This enables an accurate account of the contribution of the first coordination sphere to SCO, notably the interplay between ΔH and ΔS and the relative importance of relativistic effects, dispersion, vibrational entropy, and zero-point energies to the SCO process. As shown, these thermodynamic state functions can be described accurately with standard methods, i.e. most of the experimental solution-state SCO thermodynamics arise from the first coordination sphere (in solid-state SCO, lattice effects would have to be included separately).

Methods.

Experimental Data Set Compilation. The literature was searched for iron complexes reported to exhibit SCO nature fulfilling the requirements that i) the structure was a mono-nuclear iron complex; ii) the experimental structure was either known directly or known for a closely related analog; iii) the structure was simple enough to be modeled; and iv) thermochemical data for both ΔH and ΔS of the spin transition could be found in the literature.

The obtained data set fulfilling these criteria contain thermochemical data for both ΔH and ΔS for 30 iron(II) complexes (Table 1): **1**: $[Fe(papth)_2]^{2+}$,[39] **2**: $[Fe(tacn)_2]^{2+}$,[40] **3**: $[Fe(2\text{-}amp)_3]^{2+}$ (with ClO_4^-),[41] **4**: $[Fe(HB(pz)_3)_2]$,[42] **5**: $[Fe(pybzimH)_3]^{2+}$,[43] **6**: $[Fe(pyimH)_3]^{2+}$,[43] **7**: $[Fe(6\text{-}Mepy)_2(py)tren]^{2+}$,[44] **8**: $[Fe(tppn)]^{2+}$,[45] **9**: $[Fe(tpchxn)]^{2+}$,[45] **10**: $[Fe(ppa)_2]^{2+}$,[45] **11**: $[Fe(phen)_2(NCS)_2]$[46] and its selenocyanate analog **12**: $[Fe(phen)_2(NCSe)_2]$,[46] **13**: $[Fe(2\text{-}pic)_3]^{2+}$,[46] **14**: $[Fe(bt)_2(NCS)_2]$,[47] **15**: $[Fe(bzimpy)_2]$,[48] **16**: $[Fe(py)_2phen(NCS)_2]$,[49] **17**: $[Fe(py)_2bpym(NCS)_2]$,[49] **18**: $[Fe((NH_2)_2sar)]^{2+}$,[50] **19**: $[Fe(HC(pz)_3)_2]^{2+}$,[51] **20**: $[Fe(HC(3,5\text{-}Me_2pz)_3)_2]^{2+}$,[52] **21**: $[Fe(tp[10]aneN_3)]^{2+}$,[53] **22**: $[Fe(lpp[9]aneN_3)]^{2+}$,[54] **23**: $[Fe(btpa)]^{2+}$,[55] and **24**: $[Fe(tptMetame)]^{2+}$,[56] as well as for the iron(III) complexes **25**: $[Fe(acac)_2trien]^{+}$,[57] **26**: $[Fe(bzac)_2trien]^{+}$,[57] **27**: $[Fe(bzacCl)_2trien]^{+}$,[57] **28**: $Fe(tfac)_2trien]^{+}$,[57] **29**: $[Fe(acpa)_2]^{+}$,[58] and **30**: $[Fe(3\text{-}MeO\text{-}salenEt)_2]^{+}$.[59] We also included the strictly low-spin $[Fe(phen)_3]$ complex as control (**31**).

Chemical Models. Starting geometries used for computation were taken from the Cambridge structure database[60], when available, or modeled by simple modifications of experimental structures of closely related compounds. The equilibrium structures of both HS and LS states of all 31 complexes are given in Supporting Information, Table S1, in xyz format. In some cases, data for multiple counter ions have been reported; differences between these data are generally within the standard error of the applied methods; and since the nature of solvation of the ion pairs and the concentration of samples

cannot be modeled in a simple way, only one data point (the median for odd data numbers; otherwise the experimental number closest to the median) was chosen for each of these cases.

Table 1. The SCOFE30 data set. Experimental ΔH and ΔS for 30 spin crossover iron complexes[a].

#	Name	Metal ion	Solvent	ΔH (kJ/mol)	ΔS (J/molK)	Ref.	ΔH/ΔS [b]
1	$[Fe(papth)_2]^{2+}$	Fe^{2+}	H_2O	16.4 ±0.4	61.9 ±1.3	39	265
2	$[Fe(tacn)_2]^{2+}$	Fe^{2+}	D_2O	23.8 ±1.0	68.2 ±2.8	40	349
3	$[Fe(2\text{-}amp)_3]^{2+}$ (ClO_4^-)	Fe^{2+}	$CH_3CN–H_2O$	21.3 ±1.3	71.1 ±8.4	41	300
4	$[Fe(HB(pz)_3)_2]$	Fe^{2+}	CH_3COCH_3	16.1	47.7	42	338
5	$[Fe(pybzimH)_3]^{2+}$	Fe^{2+}	$CH_3CN– CH_3OH$	21.3 ±1.7	92.0 ±7.1	43	232
6	$[Fe(pyimH)_3]^{2+}$	Fe^{2+}	$CH_3CN– CH_3OH$	15.5 ±0.8	52.7 ±1.7	43	294
7	$[Fe(6\text{-}Mepy)_2(py)tren]^{2+}$	Fe^{2+}	CH_3COCH_3	11.9 ±1.6	35.6 ±6.3	44	334
8	$[Fe(tppn)]^{2+}$	Fe^{2+}	DMF	25.4 ±1.2	71 ±5	45	358
9	$[Fe(tpchxn)]^{2+}$	Fe^{2+}	DMF	21.1 ±1.0	62 ±3	45	340
10	$[Fe(ppa)_2]^{2+}$	Fe^{2+}	CH_3COCH_3	20.3 ±2.0	52 ±5	45	390
11	$[Fe(phen)_2(NCS)_2]$	Fe^{2+}	---	8.6 ±0.1	48.8 ±0.7	46	176
12	$[Fe(phen)_2(NCSe)_2]$	Fe^{2+}	---	11.6 ±0.4	51.2 ±2.3	46	227
13	$[Fe(2\text{-}pic)_3]^{2+}$	Fe^{2+}	H_2O	17.1	59.4	46	288
14	$[Fe(bt)_2(NCS)_2]$	Fe^{2+}	---	9.6 ±0.7	54.5 ±4.0	47	176
15	$[Fe(bzimpy)_2]$	Fe^{2+}	---	15.7 ±2.4	38.9 ±6.0	48	404
16	$[Fe(py)_2phen(NCS)_2]$	Fe^{2+}	---	3.7 ±0.5	37 ±5	49	100
17	$[Fe(py)_2bpym(NCS)_2]$	Fe^{2+}	---	6.5 ±0.5	56 ±4	49	116

18	$[Fe((NH_2)_2sar)]^{2+}$	Fe^{2+}	CD_3CN	12	30	50	400
19	$[Fe(HC(pz)_3)_2]^{2+}$	Fe^{2+}	CH_3CN	18	53	51	340
20	$[Fe(HC(3,5\text{-}Me_2pz)_3)_2]^{2+}$	Fe^{2+}	DMF	20	58	52	345
21	$[Fe(tp[10]aneN_3)]^{2+}$	Fe^{2+}	CH_3CH_2CN	23.6	84	53	281
22	$[Fe(lpp[9]aneN_3)]^{2+}$	Fe^{2+}	CH_3OH	17.1	59	54	290
23	$[Fe(btpa)]^{2+}$	Fe^{2+}	CH_3OH	27.6	89	55	310
24	$[Fe(tptMetame)]^{2+}$	Fe^{2+}	CH_3CH_2CN	19.4	85	56	228
25	$[Fe(acac)_2trien]^{+}$	Fe^{3+}	CH_3COCH_3	8.4 ±0.3	43.6 ±1.4	57	193
26	$[Fe(bzac)_2trien]^{+}$	Fe^{3+}	CH_3COCH_3	10.3 ±0.3	42.4 ±1.3	57	243
27	$[Fe(bzacCl)_2trien]^{+}$	Fe^{3+}	CH_3COCH_3	2.8 ±0.4	8.3 ±1.5	57	337
28	$Fe(tfac)_2trien]^{+}$	Fe^{3+}	CH_3COCH_3	3.2 ±0.4	5.3 ±1.7	57	604
29	$[Fe(acpa)_2]^{+}$	Fe^{3+}	---	7.0	36.2	58	193
30	$[Fe(3\text{-}MeO\text{-}salenEt)_2]^{+}$	Fe^{3+}	---	5.9	36.6	59	161

[a] Abbrevations: papth = bis(2-(2-pyridylamino)-4-(2-pyridyl)thiazole); tacn = 1,4,7-Triazacyclononane; 2-amp = tris(2-(aminomethyl)pyridine); $HB(pz)_3$ =(hydro-tris(1-pyrazolyl)borate); pybzimH = 2-(2′-pyridyl)benzimidazole; pyimH = 2-(2′-pyridyl)imidazole; 6-Mepy)$_2$(py)tren = tris(4-[(6-Me)-2-pyridyl]-3-aza-3-butenyl)amine; tppn = N,N,N′,N′-tetrakis(2-pyridylmethyl)-1,2-propanediamine; tpchxn = N,N,N′,N′-tetrakis(2-pyridylmethyl)-1*R*,2*R*-cyclohexanediamine; ppa = N′-(2-pyridylmethy1)picolinamidine; phen = 1,10-phenanthroline; NCS = thiocyanide; NCSe = selenocyanide; 2-pic = 2-aminomethylpyridine (2-picolylamine); bt =2,2′-bi-2-thiazoline; bzimpy = 2,6-bis(benzimidazol-2-yl)pyridine; py = pyridine; bpym = 2,2′-bipyrimidine; sar = 3,6,10,13,16,19-hexa-azabicyclo[6.6.6]icosane; $HC(pz)_3$ = tris-(1-pyrazolyl)-methane; HC(3,5-Me2 $pz)_3$ = tris-(3,5-dimethyl-1-pyrazolyl)-methane; tp[10]aneN_3 = N,N',N''-tris(2-pyridylmethyl)-l,4,7-triazacyclodecane; lpp[9]aneN_3 =1-(6-methyl-2-pyridylmethyl)-4,7-bis-(2-pyridylmethyl)-1,4,7-triazacyclononane; btpa = N,N,N',N'-tetrakis(2-pyridylmethyl)-6,6'-bis(aminomethyl)-2,2'- bipyridine; tptMetame = 1,1,1-tris((*N*-(2-pyridylmethyl)-*N*-methylamino)methyl)ethane; acac = acetyl-acetonate-triethylenetetramine; bzac = benzoyl-acetonate-triethylenetetramine; acpa = N-(1-acetyl-2-propylidene)-2-pyridylmethylamine; 3-MeO-salenEt = 3-methoxysalicylaldehyde-N-ethylethylenediamine. [b] As an estimate of $T_{½}$.

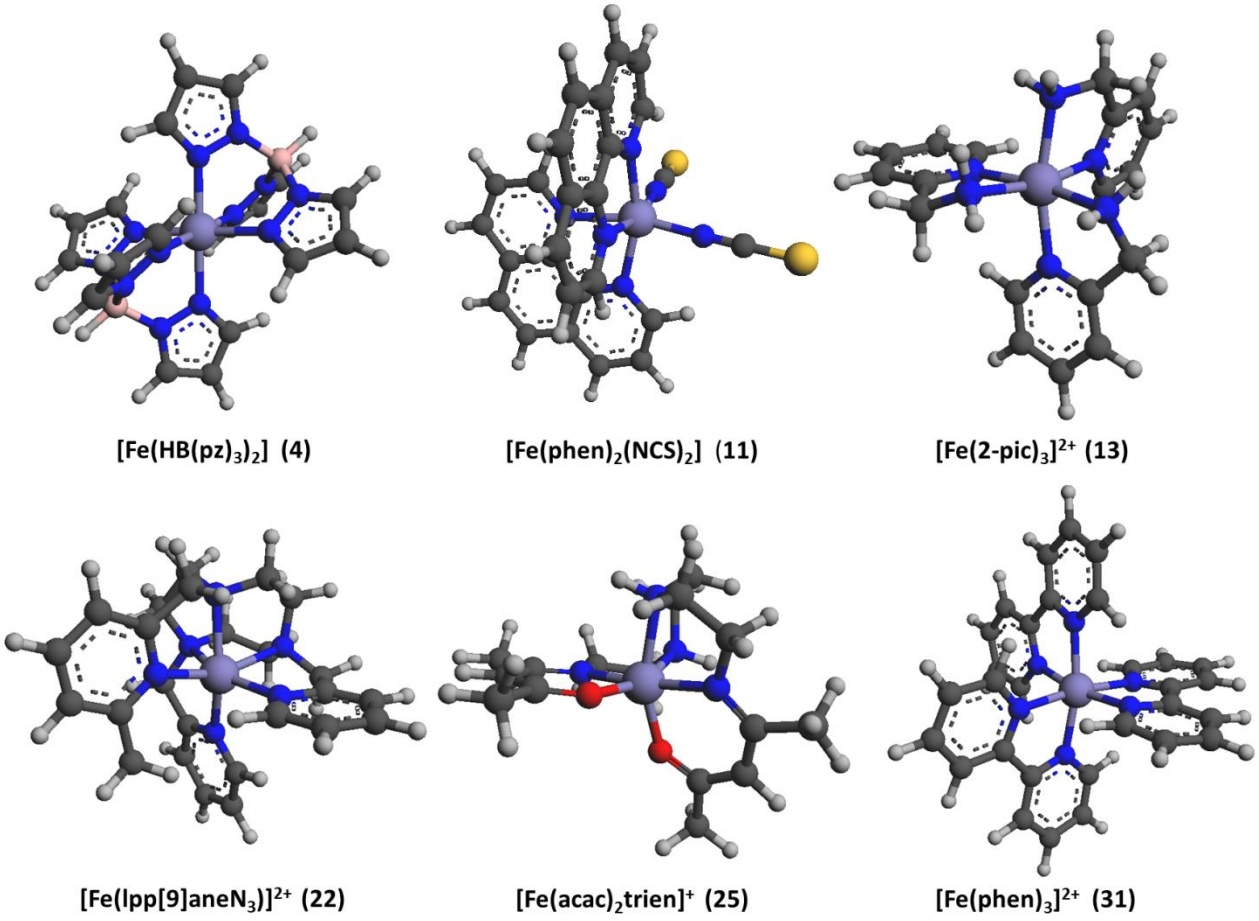

Figure 1. Representative examples of iron complexes studied in this work. Optimized coordinates of all 62 states (31 complexes in HS and LS states) can be found in the Supporting Information, Table S1.

Geometry Optimizations. The calculations were performed with the Turbomole software, versions 6.3 and 7.0.[61,62] All models were studied both in the HS state and in the LS state. We optimized the geometry of both states of all models using internal redundant coordinates to accelerate computation[63] at the BP86/def2-SVP level[64] using the Cosmo solvation model[65]: The choice of functional and basis set beyond this level has generally little effect on the geometries of metal complexes (a few picometers change in metal-ligand bond lengths), and very little effect on the relative energies, since both states are affected by a change of method in the same direction[66,67]. Condense

phase screening improves the accuracy of geometries of charged metal clusters[68], and some of the iron complexes have +2 charges, i.e. geometry optimization in a screened environment is important. Dielectric constants were used corresponding to the solvent of the experimental thermochemical data for each complex: 80 for H_2O, 20 for CH_3COCH_3, 37 for $CH_3NCHOCH_3$ (formamide), 38 for CD_3CN or CH_3CN, 28 for CH_3CH_2CN, 33 for CH_3OH, and a composition-weighted average for H_2O–CH_3CN and CH_3CN–CH_3OH mixtures. Radii of 2.0 Å for C, 1.83 Å for N, 1.72 Å for O, 1.3 Å for H, 1.5 Å for B, and 2.0 Å for Fe were applied.

When using Cosmo via Turbomole, the screening charges are calculated in every cycle and included into the Hamiltonian, i.e. both the molecular orbitals and the screening charges are optimized. For the numerical frequencies, the cavity is set up for each distorted geometry so that the segments change with geometry. This is, as everything else in quantum chemistry, not exact, but the procedure provides realistic estimates of the screening effect on bond lengths and ZPEs, and the calculations are numerically stable without oscillations that would arise from artifacts in the cavity setup.

Energy Calculations. The energy of each spin state of each complex was subsequently computed using the fully polarized, balanced basis set def2-TZVPP[69] with electronic energies converged to 10^{-7} a.u. These energies were computed with 12 density functionals: B3LYP[70,71,72,73], B3LYP*[74,75], BP86[76,77], BLYP[71,76], BHLYP, B2PLYP, B97−D[78,79], PBE[80] and PBE0[81], TPSS, TPSSh[82,83], and PW6B95[84]. B3LYP is the most widely used density functional today by an order of magnitude, as recently estimated[9]. The hybrid functionals span a range of HF exchange (10% in TPSSh, 15% in B3LYP*, 20% in B3LYP, 25% in PBE0, 50% in BHLYP) that can then be separated from the remaining exchange and correlation functional via the non-hybrid counterparts (BLYP, PBE, TPSS). In total, 31 systems were studied in two states with 12 methods, for a total of 744 energy calculations.

Dispersion effects were in all cases estimated for the single-point energies using the D3 correction[85], except B97−D, which by design contains the D2 correction and was thus not studied with additional dispersion corrections. Dispersion corrections such as D3 improve the description of relative energies of chemical systems and geometries of large, flexible molecules and van-der-Waals complexes[86,87,88]. For metal complexes, other effects such as the functional have similar effects on metal-ligand bond lengths complicate matters[89]: For example, uncorrected non-hybrids (e.g. BP86) work well in some cases whereas hybrids with high HF exchange percentages improve geometries when adding dispersion[89,90,91], probably because the 20% HF exchange tends to produce too long metal-ligand bonds[66] whereas dispersion tends to shorten them[90].

After convergence of the def2-TZVPP states in Cosmo, scalar-relativistic energies were calculated for all states, as these are sometimes significant even in first-row transition metals[66]. These were computed using the Cowan-Griffin operator[92] as implemented in Turbomole, to assess its effect on SCO. The spin orbit coupling is of the order of ~1 kJ/mol for atomic iron[93], so scalar-relativistic corrections are expected to dominate the relativistic corrections for these systems. Yet, in order to confirm this, full two-component relativistic energies were computed for 10 selected complexes, including the archetypical SCO complex **11**, using the Douglas-Kroll-Hess formalism[94,95] as implemented in Turbomole, both including spin-orbit coupling and without, and with both the orders 2 and 4[96], using the PBE functional. Special basis sets (dhf-TZVP-2c) were applied[97], and the energies thus had to be converged from scratch for both HS and LS states. The corresponding non-relativistic energies with these basis sets were also computed for both HS and LS states. For these systems, the calculations require large damping (> 1.0) and orbital shifts (0.5−1.0) to reach convergence, which increases the risk of local minima; thus, the energies had to be re-optimized afterwards without the forced convergence, in some cases started from other spinors (e.g. those from more polarized hybrid functional calculations).

Zero-Point Vibrational Energy and Entropy Estimates. The frequencies of the 31 HS and 31 LS geometry optimized states were computed numerically using the NumForce script at the BP86-def2-SVP level, the same level as the geometry optimization with Cosmo solvation. The ZPEs of HS and LS states were subtracted from these calculations and added to the energy difference between HS and LS, ΔE. The vibrational entropies and the enthalpy corrections of each spin state of each complex were obtained from thermodynamic calculations at 298 K using the freeh script of Turbomole and a scale factor of 0.9914. It was assumed that the temperature-dependence of the thermodynamic state functions from 298 K to the experimental temperature was negligible. We were interested in the difference in vibrational energy levels between HS and LS; these differences are only weakly affected by method / scaling (a scale factor change from 0.95 to 1 would e.g. change a differential ZPE of 10 kJ/mol typical of this work by 0.5 kJ/mol).

Results and Discussion.

The Nature of Entropy-Enthalpy Compensation in SCO. The importance of entropy in SCO systems is directly evident from the temperature-dependence of the spin state, with the HS state being favored by vibrational entropy; this effect is what enables thermally induced spin crossover, although the transition in the solid phase will be affected by long-range (lattice) effects[3] , which also affect the magnitude of the entropies[98]. Also, while the entropy and enthalpy estimates determine the thermodynamics of SCO, the driven SCO transition is a kinetic non-equilibrium phenomenon whose understanding (abruptness, hysteresis, etc.) requires additional features to be explained, notably an account of complex long-range interactions. Yet, no systematic attempt has been made to understand the quantitative relationship between ΔH and ΔS of SCO. From the theoretically expected inverse

relationship between the strength and entropy of a chemical bond, a compensation is expected between ΔH and ΔS in SCO if this important process is mainly driven by changes in the metal-ligand bonds, and it is known for each case individually that the entropy tends to counteract the stability of the LS state, which is otherwise energetically favored[9,24]. A recent computational attempt to define the thermochemical spin preference series vs. ligand and metal ion type[25] found that stronger ligands, which energetically tend to favor LS more, are associated with larger losses of vibrational entropy, consistent with the simple harmonic potential view, where stronger bonds have less entropy. Therefore, it is of interest to identify any general entropy-enthalpy compensation as this could be an important control parameter of SCO.

The entropy-enthalpy compensation of the systems can be quantified by plotting the reported experimental ΔS vs. ΔH, as done in Figure 2, left. This produces a linear regression with $R = 0.82$ ($R^2 = 0.68$) that is highly statistically significant ($p = 0.002$). From this comparison, one can conclude that entropy-enthalpy compensation is a very strong and general feature of SCO systems, and that it extends beyond the individual case to series of compounds, which is a finding with implications for future rational design of SCO systems. The compensation arises from the relation between weaker bond enthalpy and associated more accessible vibrational states in the high-spin state where the occupation of the e_g orbitals is favored at high temperature due to the TΔS term.

A second important observation is that the thermochemical parameters of the iron(III) and iron(II) complexes fall into two distinct groups, with the first having smaller values of ΔH and ΔS: The average ΔH and ΔS values are 6.3 kJ/mol and 28.7 J/molK for the iron(III) complexes, but 16.8 kJ/mol and 59.1 J/molK for the iron(II) complexes. This important difference is due to the weaker ligand field of the iron(III) complexes that lead to a larger entropy-enthalpy compensation. In other words, iron(III) favors LS more than iron(II), which is text-book knowledge and arises from the stronger ionic

component of the metal-ligand bonds (however, in general, one may assume that as one divides systems more and more into subsets that resemble each other more, correlation will tend to increase because of the removal of non-systematic contributions to the entropy-enthalpy compensation). The ligand strength must thus be weaker in the iron(III) systems to maintain SCO, and this means that the entropy-enthalpy compensation changes magnitude. Whereas the slope of the regression line is 2.41 for the full data set, it is in fact 1.97 for the iron(II) complexes and 5.41 for the iron(III) complexes. This finding has implications for the design of SCO systems with non-traditional combinations of ligands and metal ions.

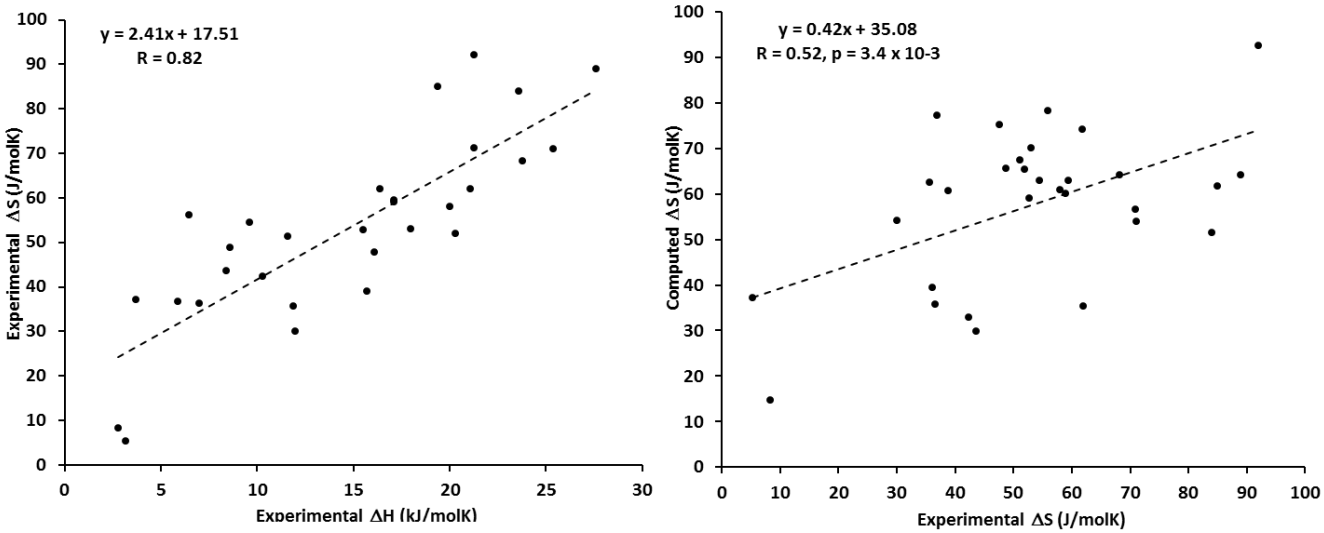

Figure 2. Left: Entropy-enthapy compensation for experimental data collected in the data set (units of J/molK). **Right:** Experimental vs. computed changes in entropies during spin crossover (J/molK).

Vibrational Entropies Can be Computed with Good Accuracy. From the compiled literature, it can be seen that vibrational TΔS of the iron SCO complexes is, as a whole, 15.8 ± 6.2 kJ/mol at 298.15 K. The favoring of HS follows directly from the occupation of the e_g orbitals and the associated longer and weaker metal-ligand bonds[8]. At thermal equilibrium relevant to most studies of

coordination chemistry, neglecting this systematic entropy may lead to erronous conclusions regarding the spin state[9]. The question is then if we can compute this entropy effect with any reasonable accuracy; there are no benchmarks on this question. However, Brehm et al.[98] have studied the vibrational entropy contribution to SCO and estimated the lattice effect from explicit solvent molecules for the archetypical SCO complex $Fe(phen)_2(NCS)_2$ (compound 11 in Table 1).

Figure 2 right shows the experimental ΔS values vs. the entropies obtained from numerically computed frequencies with the Cosmo model, using the structures optimized at the same level of theory (BP86/def2-SVP/Cosmo). It can be seen that there are substantial random errors in the regression plot, providing a standard deviation of 14.6 J/molK, corresponding to a standard error in TΔS of ~4.4 kJ/mol at room temperature. Yet, the average experimental and computed ΔS values are remarkably similar, 53.0 and 57.5 J/molK, and almost four times larger than the standard deviation; furthermore, all the computed entropies provide the physically correct direction, with high statistical significance ($p \sim 3.4 \times 10^{-3}$).

These computations show that we can satisfactorily compute vibrational entropies from frequency calculations in dielectric solvent when modelling inorganic chemistry. Including them clearly improves the prediction of free energies of electronic states vs. the alternative, to neglect entropies. A leave-two-out analysis improves *R* from 0.52 to 0.62 for 28 complexes showing that without challenging cases, better performance can be expected, so the inclusion of ΔS is generally recommended. It also shows that the first coordination sphere contributes most of the entropy of SCO, meaning that long-range entropy effects must contribute a minor part of the total entropy.

Zero-Point Energy and Thermal Effects on the Spin State Balance. The inherently quantum mechanical vibrational ZPEs contribute to the spin state balance: The ZPE is smaller for HS states than for LS states, due to the weaker metal-ligand bonds. This causes the differential ZPE to favor HS

states[9,25]. ZPE corrections are particular important for complexes with strong or moderate ligands (e.g. N-ligands, CO, and CN^-) as is the case for the iron(II) SCO complexes, and less so for weak ligands[25].

The computed ZPE corrections to the ΔE are shown in the first panel of Figure 3A. This effect always favors HS, as expected. The average effect of ZPE is 9 kJ/mol, fairly constant across all 30 systems, because of the similarity in ligands and metal ions. There is no substantial difference between the iron(III) and iron(II) complexes.

From the numerically calculated frequencies, the vibration state function and associated thermodynamic functions G, S, and H can be calculated (the freeh script of Turbomole was applied to this end). The numerical values of these corrections are shown in Supporting Information, Table S2. Figure 3A shows these thermochemical corrections in kJ/mol at 298.15 K. The ΔH corrections to the electronic energies are relatively small, because the Δ(PV) term is generally small in condense phase. However, the entropy corrections, as discussed above, cause a substantial correction to the free energy estimate of SCO, almost doubly as large as the ZPE effect.

This is not only relevant when modeling SCO systems but also when comparing HS and LS states in enzymes or transition metal catalysts, where many "energy profiles" completely ignore vibrational entropy despite changing between HS and LS and other loose vs. dense electronic states. Even more problematic cases arise if there are consecutive bond formations or bond cleavages involved, which is not the case in the simple SCO process; yet, entropy calculations can relatively well handle such cases as well, e.g. O_2 binding to heme where both spin state change and ligand binding occur simultaneously[99]. Neglect of entropy produces energies that artificially favor LS too much, although this may be partly cancelled by e.g. neglecting dispersion which, as shown below, favors LS significantly, or by using a method that intrinsically overstabilizes HS, such as a hybrid functional with too much HF exchange[9].

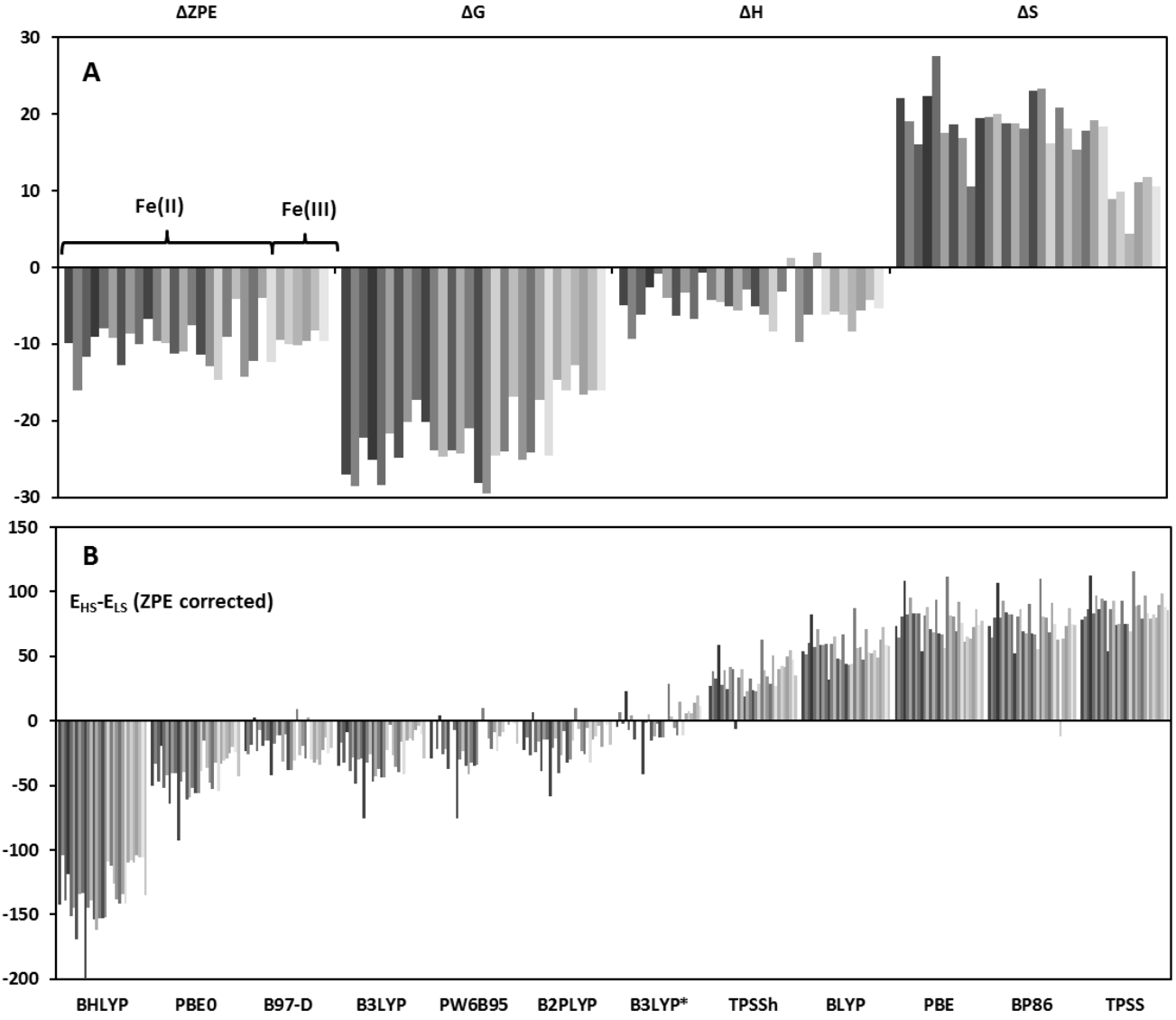

Figure 3. A) Thermochemical corrections to ΔG for individual complexes, divided into ZPE, total free energy, enthalpy, and entropy corrections, in kJ/mol. B) Enthalpies of 30 spin crossover complexes computed with 12 functionals (TZVPP energies corrected for zero-point energy and thermal enthalpy corrections, in kJ/mol).

Effect of Density Functional on Computed Enthalpies of SCO. Having now accounted for the importance of including ZPE and thermochemical corrections to SCO, the use of different methods

can be considered. Figure 3B shows the ZPE-corrected ΔH values for 12 different functionals used in this work. Since the main goal was to understand the physics of the problem, the functionals were chosen to cover a range of design principles and HF exchange fractions in hybrids, including double hybrids (B2PLYP), meta functionals (PW6B95, TPSS), meta hybrid (TPSSh), GGA hybrids (PBE0 and B3LYP), and a range of different basic exchange and correlation functionals, to sort out this effect from the HF exchange effect. Of these, B3LYP* has been designed specifically for this problem with 15% HF exchange and is expected to be relatively accurate[12,74], and TPSSh has previously been reported to exhibit high accuracy for first-row transition metal systems[100,101], including experimental enthalpies of SCO of cobalt and iron systems[16,102] and metal-ligand bond dissociations[103]. Non-hybrid functionals favor LS states, compared to hybrid functionals, a well-known consequence of HF exchange producing polarized electron densities with energy bias towards HS states[12,13].

First, the correlation functionals are compared most easily in the non-hybrids where the effect of HF exchange is absent: From Figure 3B, it can be seen that ΔE/ΔH produced by PBE and BP86 are quite similar (within 5 kJ/mol in ΔE in general). The meta GGA functional TPSS provides the strongest bias towards LS and the bias is 7 kJ/mol larger than BP86 and 11 kJ/mol larger than PBE on average. Most interestingly, the LYP correlation functional substantially favors HS relative to the other correlation functionals, by 11 kJ/mol more than PBE and 15 kJ/mol more than BP86; this effect is thus relatively important.

After the non-hybrids, the TPSSh and B3LYP* functionals follow in the middle of the range with substantially more tendency to stabilize HS, as expected because of the 10% and 15% HF exchange, respectively. For TPSS, 10% HF exchange gives ~50 kJ/mol stabilization of HS, and the effect is linear, as shown first by Reiher et al[74]. Then follows the double hybrid B2PLYP with substantiall more HS stabilization (24 kJ/mol more than B3LYP* on average). Despite the high HF

exchange fraction of 53% the HS bias is largely reduced by the MP2 correlation energy that works to compensate the pure HS bias of the slater determinant. The moderate behavior of B2PLYP for SCO is consistent with previous calculations on related systems[104] that however did not include thermochemical corrections and direct comparison to experimental ΔH and ΔS (if ΔS corrections are included in that study, the conclusions change and B2PLYP becomes less accurate than e.g. TPSSh).

As seen in Figure 3B, B2PLYP performed almost identically to the meta hybrid functional PW6B95 that was developed for thermochemistry[84], although there are differences for specific complexes. B3LYP was only slightly more HS-stabilizing than these two functionals and performed very similar to B97-D, which uses the early dispersion correction by Grimme[79]. At 15 kJ/mol more stabilization towards HS came PBE0, the much used hybrid with 25% HF exchange, and finally, with substantial HS stabilization, on average 90 kJ/mol more than PBE0, came the BHLYP hybrid with 50% HF exchange. Figure 3B thus illustrates three main effects: i) the strongest and most well-known effect of HF exchange favoring HS, ii) the not well-known effect of LYP favoring HS vs. other correlation functionals such as PBE and P86, and iii) the large compensating effect of the MP2 energy in double hybrids that counteracts the HF exchange. These various effects coincidentally cause B97-D, B3LYP, B2PLYP, and PW6B95 to behave very similar when computing ΔH for SCO.

As a control used to test for "false positives", the strictly low-spin non-SCO complex $[Fe(phen)_3]^{2+}$ was also computed. Only BHLYP produced lower energies for HS for this complex. However, when adding entropy that favors HS, also PBE0 was seen to produce too small energies in favor of LS (7 kJ/mol, thus predicting a free energy in favor of HS when adding TΔS). This illustrates the importance of including the entropy when estimating the true spin state of a molecular system.

Dispersion Substantially Affects Spin Balance by Favoring LS. Dispersion is now included in many functionals via specific corrections, and this allows one to study the effect of this second-order

instantaneous induced-dipole interaction on the process of interest. For large, polarizable electron densities changing location close in space (e.g. dissociation of bulky groups such as in B_{12}-systems[105]), dispersion is clearly important. However, even for the relative energies of spin states, there are previous indications that dispersion may be important[24,25]. Thus, to understand the physics of SCO, one needs to estimate the role of dispersion.

In this work, dispersion contributions within the first coordination sphere have been estimated; long-range effects and compensatory interactions with an explicit solvent will also contribute, but these are not studied in the present work as this issue is a general problem of theoretical chemistry that remains to be solved: When molecular packing in condense phase affects the two relevant states differently (here LS and HS) an additional error will arise from compensatory interactions with the solvent molecules or other solutes. For many normal reactions the differential compensation between the two states may be small, but for some reactions, notably bond cleavage and bond breaking reactions where the molecular volume of reaction changes substantially, the effect can be large; thus this issue has been studied in particular in the case of Co−C bond cleavage reactions of bulky cobalamins[105,106]. The only viable solution to this ongoing problem is, in this author's opinion, a fully solvated system that includes all compensatory solvent-solvent and solvent-solute interactions without cutoffs, studied by QM/MM and with adequate phase space sampling of the many possible solvent molecule alignments contributing to specific solvation within the first two or three solvation spheres.

Yet, for the current study, dispersion effects within the first coordination sphere provide a first estimate of the total dispersion contribution to SCO for a number of systems large enough to make any general conclusions. To this end, all the 31 systems were also studied with 11 functionals where D3 dispersion by Grimme[85] was included when computing the energies (B97-D already has dispersion and was thus not studied with additional D3).

Figure 4, top, shows the resulting ΔH values including ZPE, D3, and thermal enthalpy corrections. Compared to Figure 3, a substantial and fairly constant change is observed in favor of the LS state. The specific system- and method-dependent D3 corrections are visualized in Figure 4 bottom. On average across all complexes, the stabilization effect on LS amounts to 9 kJ/mol. The system-wise standard deviations are 4.3 kJ/mol, whereas the method-wise standard-deviation is 5.2 kJ/mol. Thus, dispersion corrections for SCO systems are to some extend both method-dependent and system-dependent.

The largest D3 corrections are seen for the non-hybrids BP86 and BLYP. This effect is caused by differences in the specifically parameterized D3 parameters of the individual methods[79]. The largest dispersion-corrections averaged over methods are seen for systems **5**, **15**, and **20**. All these three systems have bulky N-containing ring ligands whose interactions are larger in the smaller LS state and thus favored more by the attractive dispersion in these systems. This dispersion effect favoring LS in particular in crowded SCO systems is important to consider in rational design as it amounts to 18 kJ/mol for these systems.

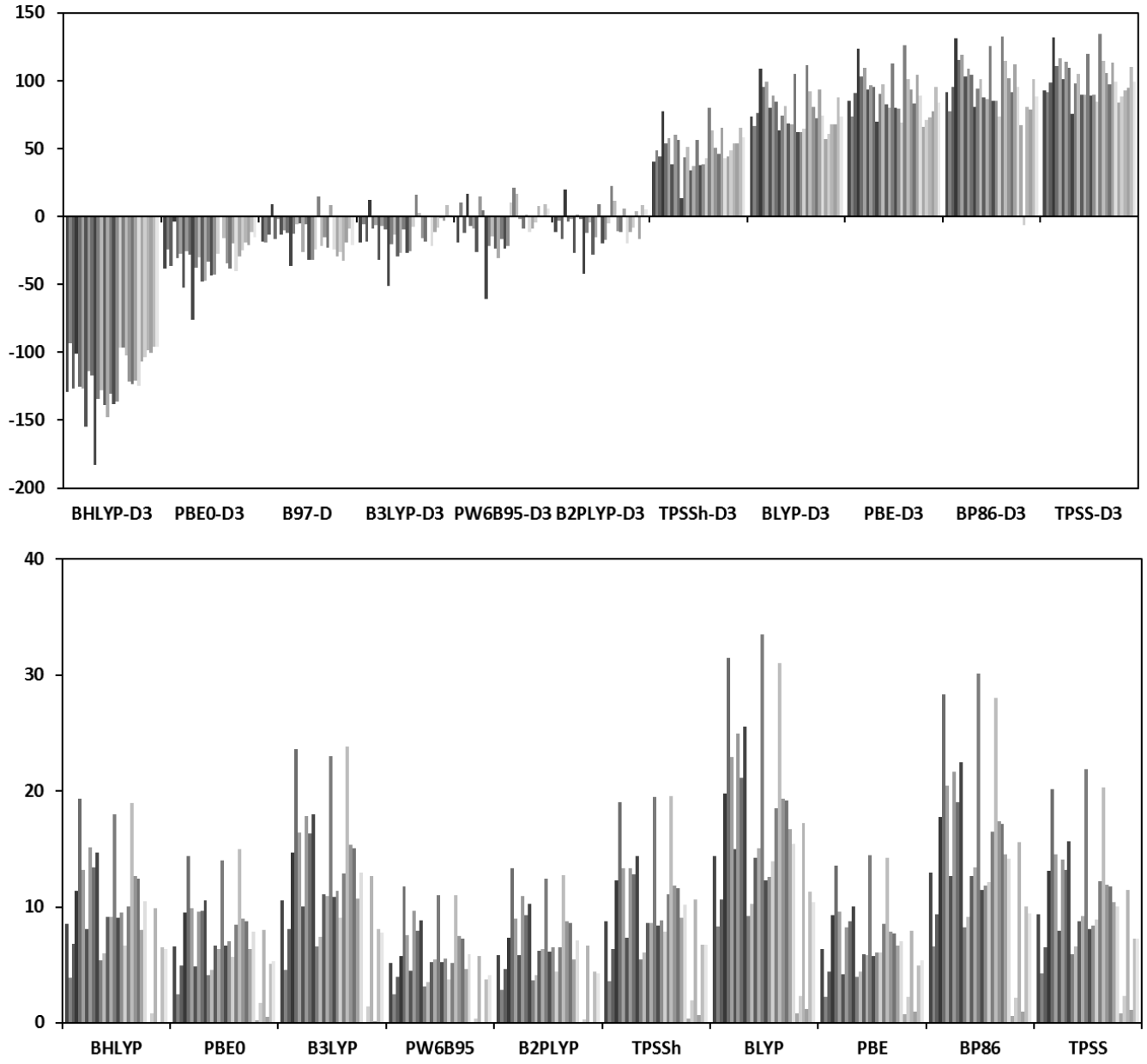

Figure 4. Top: Enthalpies of 30 spin crossover complexes computed with 11 dispersion-corrected functionals in kJ/mol (TZVPP energies corrected for zero-point energy, dispersion, and thermal enthalpy corrections). Bottom: Functional-specific D3 dispersion-corrections (kJ/mol), all in favor of low-spin.

Relativistic Effects Favor Low-Spin, but Less in Iron(III) Complexes. The last important feature that could change the spin state balance is relativistic effects. As noted already in research by Pyykko[107], the first-row of the d-block can be subject to non-negligible relativistic effects, with a notable example being the contraction of copper-ligand bonds. Relativistic effects stabilize and contract s-shells but then increase shielding, causing d-orbital expansion and destabilization. Substantial energetic effects already in the first row of the d-block were documented systematically in studies of the bond energies of M−L diatomics[66]. These effects are mainly scalar in nature, and the small spin-orbit coupling of iron is ~1 kJ/mol[93]. This was confirmed by computing selected complexes with the Douglas-Kroll-Hess two-component formalism of order 4, with and without spin-orbit coupling, giving corrections to the scalar relativistic energies of < 3 kJ/mol and typically ~1 kJ/mol (Supporting Information, Table S3 and Table S4). They show that order 4 and 2 give similar results for these iron complexes (typically within 0.1 kJ/mol, in one case ~1 kJ/mol), consistent with the overall small, mainly scalar corrections. The spin-orbit coupling corrections are 0−3 kJ/mol, i.e. the scalar-relativistic corrections computed with the Cowan-Griffin operator are a good approximation for iron complexes (this of course does not apply to heavier atoms where the non-scalar effects become rapidly larger).

The scalar-relativistic corrections to all energies were computed using the Cowin-Griffin operator[92], and the difference in the corrections for HS and LS states was then calculated for all methods and for all systems (31 x 12 x 2 = 744 calculations). The numerical data are compiled in Supporting Information, Table S5. Interestingly, the relativistic corrections are systematic and favor LS on average by ~9 kJ/mol. The effect is larger for iron(II) complexes (9.7 kJ/mol) than for iron(III) complexes (5.9 kJ/mol). Except from that difference, the system-dependence is very small, with system-wise standard deviation of 1.5 kJ/mol for the iron(II) complexes and 0.7 kJ/mol for the iron(III) complexes. This is consistent with a physical effect that is fully centered on the metal ion, in contrast to the dispersion effects that were more system-dependent because they play out in the general system.

Table 2. Mean Signed Errors (kJ/mol) of Computed ΔH_{SCO} for the 30SCOFe Data Set, Corrected for Dispersion, ZPE, and Scalar-Relativistic Effects.

#	BHLYP-D3	PBE0-D3	B97-D	B3LYP-D3	PW6B95-D3	B2PLYP-D3	B3LYP*-D3	TPSSh-D3	BLYP-D3	PBE-D3	BP86-D3	TPSS-D3
1	-150.6	-60.9	-43.5	-41.9	-41.3	-33.1	-12.5	17.6	49.6	61.2	67.6	69.4
2	-132.8	-64.8	-62.1	-47.3	-30.4	-42.7	-24.2	7.5	24.3	31.1	34.7	49.6
3	-158.8	-69.7	-48.7	-52.0	-45.0	-48.5	-22.1	11.1	42.1	56.5	60.6	64.8
4	-120.5	-24.1	-13.2	-8.2	-3.7	0.8	23.3	56.7	87.2	102.2	109.2	110.5
5	-156.3	-62.3	-50.8	-40.9	-38.5	-35.0	-8.6	21.5	62.4	69.8	81.8	77.8
6	-145.4	-47.0	-24.0	-26.8	-28.4	-20.6	5.6	37.5	78.2	88.6	97.4	95.7
7	-168.2	-66.4	-29.3	-46.2	-40.0	-39.9	-12.1	24.4	65.0	78.7	87.7	86.6
8	-154.3	-67.1	-53.7	-48.5	-26.2	-39.2	-18.9	22.1	46.3	54.0	66.2	67.9
9	-149.1	-61.0	-47.5	-42.8	-28.6	-33.8	-13.5	22.8	50.0	61.2	69.9	75.6
10	-210.5	-104.3	-67.2	-79.8	-88.8	-69.5	-46.1	-14.8	33.8	40.0	51.0	46.4
11	-139.7	-43.5	-20.8	-26.6	-27.5	-17.3	3.9	37.7	66.9	83.2	86.3	90.9
12	-138.9	-42.2	-20.2	-25.6	-26.4	-15.7	5.0	38.6	67.8	83.9	87.5	92.0
13	-162.0	-72.0	-31.1	-53.9	-47.6	-51.3	-19.1	9.6	43.7	57.6	62.4	64.9
14	-154.3	-54.6	-36.3	-35.1	-37.9	-21.5	-4.3	28.7	58.7	71.2	77.4	81.3
15	-148.7	-52.3	-27.5	-29.1	-35.9	-8.9	5.5	36.9	84.4	92.1	104.6	99.4
16	-133.5	-39.6	-30.4	-23.1	-19.6	-15.3	7.8	41.6	64.7	82.2	87.0	91.8
17	-137.5	-44.6	-36.5	-28.3	-23.7	-18.1	2.1	36.0	58.6	75.8	80.9	86.4
18	-112.4	-44.6	-43.2	-25.1	-6.4	-20.9	-2.4	25.2	46.5	50.8	55.3	66.5
19	-119.5	-24.4	-11.2	-8.5	5.1	-0.4	22.5	55.7	86.5	100.9	107.1	109.3
20	-130.4	-45.1	-52.7	-27.3	-12.1	-16.5	2.3	34.3	61.9	70.7	83.6	84.6
21	-158.9	-72.7	-55.0	-54.3	-39.8	-47.9	-24.5	12.2	42.0	54.4	62.4	67.4
22	-148.4	-63.8	-50.4	-44.5	-34.2	-36.1	-16.1	20.3	45.8	56.9	65.3	71.1
23	-164.7	-64.6	-39.3	-44.7	-43.3	-38.4	-13.9	20.6	46.6	58.0	64.9	67.4
24	-154.7	-70.9	-57.1	-52.9	-41.3	-49.2	-23.3	12.6	43.5	58.2	64.2	68.7
25	-120.3	-42.7	-42.1	-24.3	-21.3	-25.3	10.0	31.8	45.5	54.0	54.9	71.9
26	-120.4	-42.2	-42.7	-24.6	-21.0	-25.3	9.9	32.3	45.8	55.6	-22.0	72.7
27	-99.7	-20.6	-33.7	-1.7	6.7	2.4	32.5	53.4	68.3	73.3	80.7	93.1
28	-103.3	-23.8	-21.5	-5.4	-1.7	-19.9	29.7	52.0	66.8	75.9	76.8	93.3
29	-105.2	-20.8	-17.7	-0.6	0.0	-1.6	41.9	56.7	80.5	88.1	93.0	102.3
30	-103.2	-22.4	-27.8	-5.4	-0.6	-2.3	30.3	51.9	68.1	78.2	82.4	93.8
	Average											
	-140.1	**-51.2**	**-37.9**	**-32.5**	**-26.7**	**-26.4**	**-1.0**	**29.8**	**57.7**	**68.8**	**72.7**	**80.4**

Fully Corrected ΔH values of SCO. After having discussed these various effects separately, the paper ends by compiling the computed enthalpies of SCO with all corrections included, as shown in Table 2. These are the numbers that can be compared with the experimental enthalpies of SCO as seen in Table 1. The mean signed error from such a comparison is shown in the last row of Table 2.

From the results, it can be seen that even with vibrational and thermal corrections that favor HS, the non-hybrids that produce dense electron states and favor LS do not produce the experimental HS states comfortably, i.e. some HF exchange is needed to produce a balanced description of electron correlation in SCO systems[12,13,22].

TPSSh and B3LYP* both work well if one neglects dispersion and relativistic effects, but includes thermal and zero-point effects, as has usually been done before. When B3LYP* was recommended[74], there was no dispersion correction to account for the important effect of dispersion on SCO that is observed in this work. However, when all the physical effects are corrected for, using the dispersion correction taken from B3LYP (this correction is not very functional-sensitive so this is justified), B3LYP* performs remarkably accurate also in a fully corrected (including dispersion-corrected) context, with a signed error of only a few kJ/mol.

As a final point of interest, the linear dependence of ΔH on HF exchange is shown in Figure 5. This linearity was first observed by Reiher et al.[74], motivating the development of the B3LYP* functional. It can be seen that for the totality of the 30 SCO systems, the HS state is favored by 4.2 kJ/mol per 1% of HF exchange. However, the dependency is system-specific and ranges from 3.5 to 5.3 kJ/mol (the two extreme cases, compounds **2** and **10**), as shown in Figure 5B and 5C, respectively.

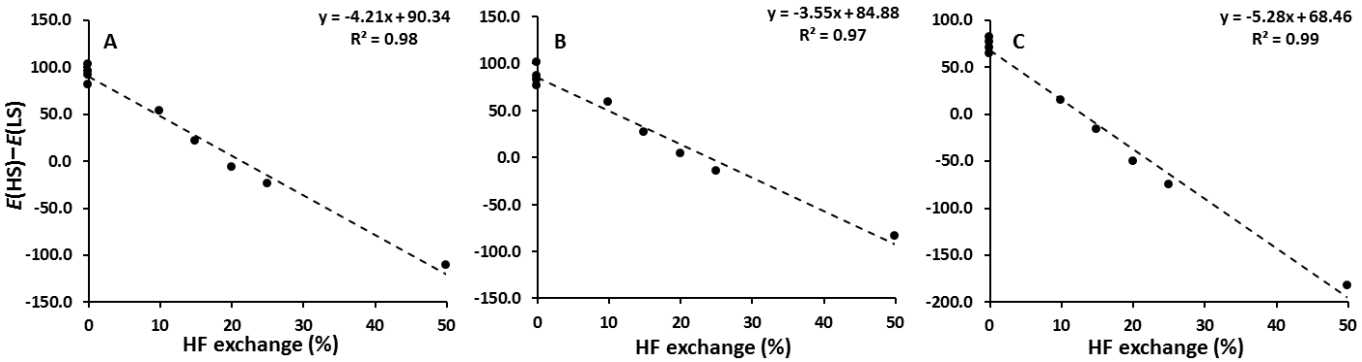

Figure 5. Energy difference (kJ/mol) between high-spin and low-spin states vs. HF exchange percentage, using BHLYP (50%), PBE (25%), B3LYP (20%), B3LYP* (15%), TPSSh (10%), and the non-hybrids TPSS, PBE, and BLYP to define 0%. A) For the total of all 30 SCO systems. B) For compound **2**; C) For compound **10** (the two systems with the most extreme dependencies)

Conclusions.

The spin balance depends on several physical effects, studied systematically in this work for the largest compilation of SCO systems so far. It is well known that entropy and enthalpy acts oppositely in SCO for individual systems, due to the LS being energetically favored but also having less vibrational entropy[9]. However, it is found here that entropy and enthalpy of SCO are highly compensatory across the SCO systems as a whole, with a remarkable correlation coefficient of R ~0.82. This conclusion was reached from compilation and regression analysis of experimental data alone.

Then, it was shown that the vibrational entropies can be computed with good accuracy if they are computed in solvent models. Thus, because of the entropy-enthalpy compensation, entropy needs to be included when estimating the spin state of a transition metal complex, including a catalytic intermediate or a SCO system.

While ZPE and vibrational entropy systematically favor HS, due to the longer, weaker bonds of the HS state with occupied e_g type orbitals, scalar-relativistic effects and dispersion effects consistently favor LS by non-negligible amounts. Dispersion favors LS on average by 9 kJ/mol, but in a system specific way, being particularly important for SCO systems with crowded ligands, because these are in closer contact in the more compact LS state. It is found that relativistic effects also favor LS by ~9 kJ/mol on average, more for iron(III) and less for iron(II) systems, and thus substantially contribute to the spin balance and SCO process, but in a less system-dependent way. The more compact LS state is

favored by the s-shell stabilization, whereas the diffuse, higher angular momentum orbitals are destabilized by the reduced nuclear charge of the more compact relativistic core.

Interestingly, these various effects tend to cancel to some extend in many systems. Cancellation of the errors from neglecting the effects studied in this work may have ended up providing reasonable results in some previous studies, but such cancellations cannot be generally relied upon, as systems will differ in terms of their relativistic, thermal, and dispersion contributions to the spin balance, since all these are system-dependent. When including all effects, B3LYP* performs remarkably accurate, with a signed error of only a few kJ/mol.

However, the main conclusion from this work is to pinpoint the magnitudes and directions of the various physical drivers of SCO, which may be of interest in future rational design of SCO systems.

Supporting Information Available. Table S1: XYZ coordinates for all geometry-optimized systems in both high-spin and low-spin states. Table S2: Electronic energies and thermochemical corrections for all studied systems. Table S3: Relativistic Douglas-Kroll-Hess and non-relativistic electronic energies (PBE/dhf-TZVP-2c). Table S4: ΔE (HS−LS) computed from energies of Table S3 (PBE/dhf-TZVP-2c), and gap corrections. Table S5: Cowan-Griffin corrections to high-spin low-spin gap for all 31 studied complexes. This material is available free of charge via the Internet at http:/pubs.acs.org.

Acknowledgements. This research has been supported by the Danish Center for Scientific Computing (Grant # 2012-02-23).

References.

(1) Scheidt, W.R.; Reed, C.A. *Chem. Rev.* **1981**, *81*, 543–555.

(2) Jensen, K. P.; Ryde, U. *J. Biol. Chem*. **2004**, *279*, 14561–14569.

(3) Gütlich, P.; Goodwin, H. A. *Top. Curr. Chem*. **2004**, *233*, 1–47.

(4) Létard, J.-L.; Guionneau, P.; Goux-Capes, L. *Top. Curr. Chem*. **2004**, *235*, 221–249.

(5) Sorai, M.; Nakano, M.; Miyazaki, Y. *Chem. Rev*. **2006**, *106*, 976−1031.

(6) Harvey, J. N.; Poli, R.; Smith, K. M. *Coord. Chem. Rev*. **2003**, *238*, 347–361.

(7) Lomont, J. P.; Nguyen, S. C.; Harris, C. B. *Acc. Chem. Res*. **2014**, *47*, 1634–1642.

(8) Toftlund, H. *Monatshefte für Chemie* **2001**, *132*, 1269−1277.

(9) Kepp, K. P. *Coord. Chem. Rev*. **2013**, *257*, 196−209.

(10) Fajans, K. *Naturwissenschaften* **1923**, *11*, 165−172.

(11) Tsuchida, R. *Bull. Chem. Soc. Jpn* **1938**, *13*, 388−400.

(12) Reiher, M. *Inorg. Chem*. **2002**, *41*, 6928−6935.

(13) Swart, M. *J. Chem. Theory Comput*. **2008**, *4*, 2057–2066.

(14) Paulsen, H.; Duelund, L.; Winkler, H.; Toftlund, H.; Trautwein, A. X. *Inorg. Chem*. **2001**, *40*, 2201−2203.

(15) Daku, L. M. L.; Vargas, A.; Hauser, A.; Fouqueau, A.; Casida, M. E. *ChemPysChem* **2005**, *6*, 1393−1410.

(16) Jensen, K. P.; Cirera, J. *J. Phys. Chem. A* **2009**, *113*, 10033−10039.

(17) Hughes, T. F.; Friesner, R. A. *J. Chem. Theory Comput*. **2011**, *7*, 19–32.

(18) Baranovic, G. *Chem. Phys. Lett.* **2003**, *369*, 668–672.

(19) Neese, F. *J. Biol. Inorg. Chem*. **2006**, *11*, 702–711.

(20) Zein, S.; Borshch, S. A.; Fleurat-Lessard, P.; Casida, M. E.; Chermette, H. *J. Chem. Phys.* **2007**, *126*, 014105.

(21) Paulsen, H.; Schünemann, V.; Wolny, J. A. *Eur. J. Inorg. Chem*. **2013**, 628–641.

(22) Pierloot, K.; Vancoillie, S. *J. Chem. Phys*. **2008**, *128*, 034104.

(23) Ioannidis, E. I.; Kulika, H. J. *J. Chem. Phys*. **2015**, *143*, 034104.

(24) Kepp, K. P. *J. Inorg. Biochem.* **2011**, *105*, 1286–1292.

(25) Mortensen, S. R.; Kepp, K. P. *J. Phys. Chem. A* **2015**, *119*, 4041–4050.

(26) Isley III, W. C.; Zarra, S.; Carlson, R. K.; Bilbeisi, R. A.; Ronson, T. K.; Nitschke, J. R.; Gagliardi, L.; Cramer, C. J. *Phys. Chem. Chem. Phys.* **2014**, *16*, 10620−10628.

(27) Houghton, B. J.; Deeth, R. J. *Eur. J. Inorg. Chem*. **2014**, 4573–4580.

(28) Andersson, K.; Malmqvist, P. Å.; Roos, B. O. *J. Chem. Phys*. **1992**, *96*, 1218−1226.

(29) Marti, K. H.; Ondik, I. M.; Moritz, G.; Reiher, M. *J. Chem. Phys.* **2008**, *128*, 014104.

(30) Halcrow, M. A. *Spin-Crossover Materials: Properties and Applications*, First Edition. John Wiley & Sons, Ltd. 2013.

(31) Deeth, R. J.; Anastasi, A. E.; Wilcockson, M. J. *J. Am. Chem. Soc*. **2010**, *132*, 6876−6877.

(32) Handley, C. M.; Deeth, R. J. *J. Chem. Theory. Comput*. **2012**, *8*, 194−202.

(33) Johnson, C. L.; Morgan, G. G.; Albrecht, M. *J. Mater. Chem. C* **2015**, *3*, 7883−7889.

(34) Lennartson, A.; Bond, A. D.; Piligkos, S.; McKenzie, C. J. *Angew. Chem.* **2012**, *124*, 11211−11214.

(35) Cirera, J.; Babin, V.; Paesani, F. *Inorg. Chem*. **2014**, *53*, 11020–11028.

(36) Cirera, J.; Paesani, F. *Inorg. Chem*. **2012**, *51*, 8194–8201.

(37) Middlemiss, D. S.; Deeth, R. J. *J. Chem. Phys.* **2014**, *140*, 144503.

(38) Middlemiss, D. S.; Portinari, D.; Grey, C. P.; Morrison, C. A.; Wilson, C. C. *Phys. Rev. B* **2010**, *81*, 184410.

(39) Beattie, J. K.; Binstead, R. A.; West, R. *J. Am. Chem. Soc.* **1978**, *100*, 3044−3050.

(40) Turner, J. W.; Schultz, F. A. *Inorg. Chem.* **1999**, *38*, 358−364.

(41) Chum, H. L.; Vanin, J. A.; Holanda, M. I. D. *Inorg. Chem*. **1982**, *21*, 1146−1152.

(42) Jesson, J. P.; Swiatoslaw, T.; Eaton, D. R. *J. Am. Chem. Soc.* **1967**, *89*, 3158−3164.

(43) Reeder, K. A.; Dose, E. V.; Wilson, L. J. *Inorg. Chem*. **1978**, *17*, 1071−1075.

(44) Hoselton, M. A.; Wilson, L. J.; Drago, R. S . *J . Am. Chem. Soc.* **1975**, *97*, 1722−1729.

(45) McGarvey, J. J.; Lawthers, I.; Heremans, K.; Toftlund, H. *Inorg. Chem.* **1990**, *29*, 252−256.

(46) Sorai M. *Bull. Chem. Soc. Jpn*. **2001**, *74*, 2223–2253.

(47) Kulshreshtha S. K.; Sasikala R. *Chem. Phys. Lett.* **1986**, *123*, 215–217.

(48) Papankova, B.; Vrbová; M.; Boča, R.; Šimon, P.; Falk, K.; Miehe, G.; Fuess, H. *J. Thermal Anal. Calorimetry* **2002**, *67*, 721−731.

(49) Claude, R.; Real, J.-A.; Zarembowitch, J.; Kahn, O.; Ouahab, L.; Grandjean, D.; Boukheddaden, K.; Varret, F.; Dworkin, A. *Inorg Chem.* **1990**, *29*, 4442–4448.

(50) Martin, L. L.; Hagen, K. S.; Hauser, A.; Martin, R. L.; Sargeson, A. M. *J. Chem. Soc. Chem. Commun*. **1988**, 1313–1315.

(51) McGarvey, J. J.; Toftlund, H.; Al-Obaidi, A. H. R.; Taylor, K. P.; Bell, S. E. J. *Inorg. Chem.* **1993**, *32*, 2469–2472.

(52) Reger, D. L.; Little, C. A.; Rheingold, A. L.; Lam, M.; Liable-Sands, L. M.; Rhagitan, B.; Concolino, T.; Mohan, A.; Long, G. J.; Briois, V.; Grandjean, F. *Inorg. Chem*. **2001**, *40*, 1508–1520.

(53) Al-Obaidi, A. H. R.; McGarvey, J. J.; Taylor, K. P.; Bell, S. E. J.; Jensen, K. B.; Toftlund, H. *J. Chem. Soc. Chem. Comm*. **1993**, 536–538.

(54) Koikawa, M.; Hazell, A.; Jensen, K. B.; McGarvey, J. J.; Pedersen, J. Z.; Toftlund, H. *J. Chem. Soc. Dalton. Trans.* **1998**, 1085–1086.

(55) Jensen, K. B. Mono and Dinuclear Iron Complexes. PhD Thesis. Department of Chemistry, Odense University, 1997.

(56) Al-Obaidi, A. H. R.; Jensen, K. B.; McGarvey, J. J.; Toftlund, H.; Jensen, B.; Bell, S. E .J.; Carrol, J. G. *Inorg. Chem.* **1996**, *35*, 5055–5060.

(57) Dose, E. V.; Murphy, K. M. M.; Wilson, L. J. *Inorg. Chem.* **1976**, *15*, 2622–2630.

(58) Sorai, M.; Maeda, Y.; Oshio, H. *J. Phys. Chem. Solids* **1990**, 51, 941–951.

(59) Sorai, M.; Burriel, R.; Westrum, Jr., E. F.; Hendrickson, D. N. *J. Phys. Chem. B*, **2008**, *112*, 4344–4350.

(60) Allen, F. H. *Acta Cryst*. **2002**, *B58*, 380–388.

(61) Ahlrichs, R.; Bär, M.; Häser, M.; Horn, H.; Kölmel, C. *Chem. Phys. Lett*. **1989**, *162*, 165–169.

(62) Treutler, O.; Ahlrichs, R. *J. Chem. Phys.* **1995**, *102*, 346−354.

(63) Arnim, M. V.; Ahlrichs, R. *J. Chem. Phys*. **1999**, *111*, 9183.

(64) Weigend, F.; Ahlrichs, R. *Phys. Chem. Chem. Phys*. **2005**, *7*, 3297–3305.

(65) Klamt, A.; Jonas, V.; Bürger, T.; Lohrenz, J. C. W. *J. Phys. Chem. A* **1998**, *102*, 5074–5085.

(66) Jensen, K. P.; Roos, B. O.; Ryde, U. *J. Chem. Phys*. **2007**, *126*, 014103.

(67) Waller, M. P.; Braun, H.; Hojdis, N.; Bühl, M. *J. Chem. Theory Comput.* **2007,** *3,* 2234–2242.

(68) Jensen, K. P.; Rykær, M. *Dalton Trans.* **2010**, *39*, 9684–9695.

(69) Schäfer, A.; Horn, H.; Ahlrichs, R. *J. Chem. Phys*. **1992**, *97*, 2571–2577.

(70) Becke, A. D. *J. Chem. Phys.* **1993**, *98*, 5648−5652.

(71) Lee, C.; Yang, W.; Parr, R. G. *Phys. Rev. B* **1988**, *37*, 785−789.

(72) Stephens, P. J.; Devlin, F. J.; Chabalowski, C. F.; Frisch, M. J. *J. Phys. Chem.* **1994**, *98*,

11623−11627.

(73) Kim, K.; Jordan, K. D. *J. Phys. Chem*. **1994**, *98*, 10089−10094.

(74) Reiher, M.; Salomon, O.; Hess, B. A. *Theor. Chem. Acc*. **2001**, *107*, 48−55.

(75) Salomon, O.; Reiher, M.; Hess, B. A. *J. Chem. Phys*. **2002**, *117*, 4729–4737.

(76) Becke, A. D. *Phys. Rev. A* **1988**, *38*, 3098–3100.

(77) Perdew, J. P. *Phys. Rev. B* **1986**, *33*, 8822–8824.

(78) Becke, A. D. *J. Chem. Phys.* **1997**, *107*, 8554–8560.

(79) Grimme, S. *J. Comput. Chem.* **2006**, *27*, 1787–1799.

(80) Perdew, J. P.; Burke, K.; Ernzerhof, M. *Phys. Rev. Lett.* **1996**, *77*, 3865–3868.

(81) Adamo, C.; Barone, V. *J. Chem. Phys.* **1999**, *110*, 6158−6169.

(82) Tao, J.; Perdew, J. P.; Staroverov, V. N.; Scuseria, G. E. *Phys. Rev. Lett*. **2003**, *91*, 146401.

(83) Perdew, J. P.; Tao, J.; Staroverov, V. N.; Scuseria, G. E. *J. Chem. Phys*. **2004**, *120*, 6898−6911.

(84) Zhao, Y.; Truhlar, D. G. *J. Phys. Chem. A* **2005**, *109*, 5656–5667.

(85) Grimme, S.; Antony, J.; Ehrlich, S.; Krieg, H. *J. Chem. Phys*. **2010**, *132*, 154104.

(86) Grimme, S. *J. Comput. Chem*. **2004**, *25*, 1463–1473.

(87) Grimme, S.; Steinmetz, M. *Phys. Chem. Chem. Phys*. **2013**, *15*, 16031–16042.

(88) Tunega, D.; Bucko, T.; Zaoui, A. *J. Chem. Phys*. **2012**, *137*, 114105.

(89) Weymuth, T.; Couzijn, E. P. A.; Chen. P.; Reiher, M. *J. Chem. Theory Comput*., **2014**, *10*, 3092–3103.

(90) Hujo, W.; Grimme, S. *J. Chem. Theory Comput*. **2013**, *9*, 308−315.

(91) Lonsdale, R.; Harvey, J. N.; Mulholland, A. J. *J. Phys. Chem. Lett.* **2010**, *1*, 3232–3237.

(92) Cowan, R. D.; Griffin, D. C. *J. Opt. Soc. Am*. **1976**, *6*, 1010−1014.

(93) Moore, C. E. *Atomic Energy Levels*, United States Department of Commerce & National Bureau of Standards, Washington, D. C. 1971. pp. 56–57.

(94) Hess, B. A. *Phys. Rev. A.* **1986**, *33*, 3742−3748.

(95) Reiher, M. *Theor. Chem. Acc.* **2006**, *116*, 241−252.

(96) Reiher, M.; Wolf, A. *J. Chem. Phys.* **2004**, *121*, 2037−2047.

(97) Weigend, F.; Baldes, A. *J. Chem. Phys*. **2010**, *133*, 174102.

(98) Brehm, G.; Reiher, M.; Schneider, S. *J. Phys. Chem. A* **2002**, *106*, 12024−12034.

(99) Kepp, K. P. *ChemPhysChem* **2013**, *14*, 3551−3558.

(100) Furche, F.; Perdew, J. P. *J. Chem. Phys*. **2006**, *124*, 044103.

(101) Jensen, K. P. *Inorg. Chem*. **2008**, *47*, 10357–10365.

(102) Matouzenko, G. S.; Borshch, S. A.; Schünemann, V.; Wolny, J. A. *Phys. Chem. Chem. Phys*. **2013**, *15*, 7411−7419.

(103) Kepp, K. P.; Dasmeh, P. *J. Phys. Chem. B* **2013**, *117*, 3755−3770.

(104) Ye, S.; Neese, F. *Inorg. Chem*. **2010**, *49*, 772–774.

(105) Kepp, K. P. *J. Phys. Chem. A* **2014**, *118*, 7104–7117.

(106) Ryde, U.; Mata, R. A.; Grimme, S. *Dalton Trans*. **2011**, *40*, 11176–11183.

(107) Pyykko, P. Relativistic Effects in Structural Chemistry. *Chem. Rev*. **1988**, *88*, 563–594.

For Table of Contents Only

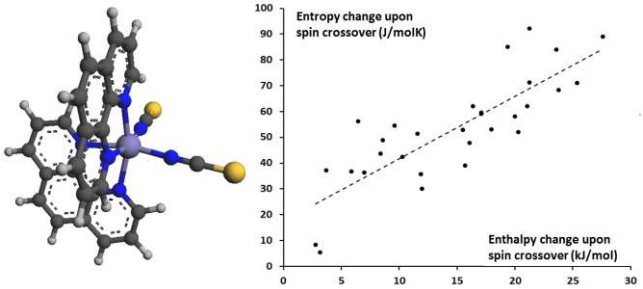

Spin crossover was studied in 30 iron complexes using density functional theory to quantify the direction and magnitude of dispersion, relativistic effects, zero point energies, and vibrational entropy. Remarkably consistent entropy-enthalpy compensation was identified. Zero-point energies favor high-spin by 9 kJ/mol on average; dispersion and relativistic effects both favor low-spin by 9 kJ/mol on average. These drivers dominate the thermodynamics (but not the transition nature) of SCO and should be considered in rational design of new spin crossover systems.